Journal of Structural Geology, Vol. 12, No. 2, pp. 177 to 184, 1990
Printed in Great Britain

0191–8141/90 $03.00+0.00

Texture development in deformed granodiorites from the Santa Rosa mylonite zone, southern California

HANS-RUDOLF WENK

Department of Geology and Geophysics, University of California, Berkeley, CA 94720, U.S.A.

and

JEAN PANNETIER

Institut Laue-Langevin, 156X, 38042 Grenoble Cédex, France

(*Received* 1 *February* 1989; *accepted in revised form* 14 *August* 1989)

Abstract—We report on texture development of granodiorite which has been progressively deformed to mylonite and phyllonite in the Santa Rosa mylonite zone in southern California. Since it is extremely difficult to measure pole figures of materials with complex diffraction patterns, it was necessary to use sophisticated neutron diffraction techniques with high resolution and position-sensitive detectors which enable the mathematical deconvolution of at least part of the spectrum. We could construct separate pole figures for biotite, quartz and plagioclase which are the major components. In the granodiorite protolith the preferred orientations of all phases are weak. In the mylonite biotite and quartz develop strong preferred orientations, whereas feldspars remain randomly oriented. Quartz has *c*-axes in the intermediate strain axis as is common in other mylonites. Interestingly, biotite *a*-axes show preferred orientation, suggesting that slip may be involved rather than just rigid body rotation. In phyllonite with a grain size of about 50 μm, the biotite fabric is very strong. However the quartz fabric has largely vanished, perhaps by superplastic processes which do not produce texture. A weak plagioclase fabric has developed.

INTRODUCTION

ROCKS which are composed of more than one phase are the most common types in the Earth's crust and in the mantle. Most investigations of the mechanical behavior of rocks have treated them as homogeneous, not considering that the various phases are generally different in strength, have different grain shapes and a different orientation distribution which changes during the course of deformation. Such a macroscopic approach which assumes homogeneity can only provide an empirical description, since mechanisms occur on the grain scale and depend on heterogeneous properties. Quantitative studies of polycrystal plasticity, not only of rocks but of metals as well, have been largely restricted to single phase materials and for these, theories such as that of Taylor (1938), have produced a wealth of information. Theoretical complexities in polyphase materials are considerable, but even worse is the lack of data. In this report we describe the preferred orientations developed in the three principal phases of granodiorite which has been progressively deformed to mylonite and phyllonite. The rocks are from the Santa Rosa mylonite zone in southern California and deformation occurred at conditions of amphibolite-facies metamorphism. We have previously documented that at this locality fabric changes are not accompanied by significant chemical or mineralogical changes (O'Brien *et al.* 1987, but see Simpson & Wintsch 1989).

SAMPLE DESCRIPTION

The three rocks chosen for this study are from the upper part of Palm Canyon south of Palm Springs, California. They belong to the Peninsular Ranges batholith and were deformed in the Santa Rosa mylonite zone in the late Cretaceous (Erskine & Wenk 1985). The deformation was dominantly ductile. A sharp transition from relatively undeformed granodiorite to mylonite and phyllonite is well exposed and easily accessible in the brushy slopes on both sides of Palm Canyon Creek south of Highway 74. In this region the plutonic part of the mylonite zone below the Palm Canyon fault is compressed from a width of 1000 m farther north to a width of less than 200 m. This may be the reason for the occurrence of extensive zones of extremely deformed phyllonites and ultramylonites which are locally up to 50 m wide (see fig. 1 in O'Brien *et al.* 1987). The rocks are granodioritic in composition, consisting of 50–55% plagioclase (An_{30}), 6–14% alkali feldspar, 25% quartz and 10% biotite (Table 1). In the undeformed granodiorite there are small amounts of chlorite, and in the mylonite there is minor epidote. During progressive deformation the most pronounced change is a reduction in grain size (Figs. 1 and 2). First quartz and subsequently biotite grains disperse into fine agglomerates, biotite partially by cataclastic processes (Goodwin & Wenk in press) but mainly through recrystallization. Feldspar crystals remain largely intact in the mylonite except for cataclas-

Table 1. Location and normative composition of samples

Sample	Location	Normative composition (weight %)				
		Biotite	Quartz	Albite	Anorthite	K-spar
PC 89 granite	116°30'37"W 33°35'10"N	10.9	22.5	35.7	19.8	5.9
PC 82 mylonite	116°30'7.5"W 33°34'50"N	9.0	24.4	31.7	17.4	14.1
PC 92 phyllonite	116°31'15"W 33°34'54"N	8.3	24.8	34.9	19.5	6.9

tic rounding of their corners (Ague 1988). Only in phyllonites and ultramylonites do feldspars break down by cataclasis and dynamic recrystallization and the grain size becomes uniformly small, giving the rock a glassy appearance in hand specimens.

In relatively undeformed granodiorite (PC 89, Fig. 2a), the grain size of quartz is 2–3 mm, that of plagioclase 1–2 mm. Even though no texture pattern is apparent in thin sections, there are signs of deformation. Quartz shows undulatory extinction and polygonization. Plagioclase, which is frequently zoned and slightly altered to sericite, is occasionally bent and fractured. Biotite is also bent with signs of cataclasis near grain margins. Alkali feldspar does not exhibit twinning.

The mylonite sample (PC 82, Fig. 2b) is representative of the bulk of the mylonite zone. Quartz has completely recrystallized and is dispersed throughout the aggregate. Its grain size is reduced to 0.05 mm, and it generally occurs in clusters of similar size as the original grain size. The gypsum plate indicates that its preferred orientation is strong. Plagioclase displays fine pericline twinning. Its grain size is slightly reduced and grain corners are rounded. The resulting fine-grained groundmass surrounding the large grains shows no apparent preferred orientation as ascertained with a gypsum plate. For biotite some porphyroclasts are preserved, but more than 80% is finely recrystallized. The sample in question contains as accessories some epidote and sphene. Both are fairly resistant to deformation.

The phyllonite (PC 92, Fig. 2c) is uniformly fine grained (<50 μm) except for occasional rounded plagioclase relics. The gypsum plate indicates weak preferred orientation of quartz and feldspars. Stringers of quartz define a *C*-foliation. A second set of shear structures is at 30° as described by O'Brien *et al.* (1987).

Oriented samples were collected in the field, and we assigned mesoscopic fabric co-ordinates based on visible foliation and lineation. In the case of undeformed granodiorite, this has been most difficult, as will become apparent in the texture analysis. Texture data are referred to these mesoscopic co-ordinates with the foliation Z representing the dominant shear plane (O'Brien *et al.* 1987), the lineation is X, and Y is perpendicular to X and Z.

On these same samples we measured elastic properties at a range of pressures and temperatures (Kern & Wenk in press). We observed at 600 MPa anisotropies of p velocities of 4% for mylonite PC82 and 11% for phyllonite PC92 which we attribute mainly to preferred orientation of biotite.

METHOD OF TEXTURE ANALYSIS

Textures of polyphase materials are inherently difficult to determine. If the grain size is sufficiently large, a universal stage on an optical microscope can be used, but this supplies only limited information on the orientation of quartz and biotite, and measuring the orientation of plagioclase is difficult. Furthermore, the grain size in our deformed samples is too small for optical investigation.

Another method, only recently applied to texture research, is that of electron microscopy, either TEM or SEM (e.g. Lloyd & Ferguson 1986, Dingley 1987, Schwarzer & Weiland 1988). This involves tedious grain by grain measurements but may become important in the future.

In recent years diffraction techniques have been most widely used, to measure pole figures of diffracting lattice planes. Unfortunately, angular resolution of X-ray pole figure goniometers and of most neutron diffraction facilities is poor (e.g. Wenk *et al.* 1984). Therefore we have made use of neutron diffraction at the high flux reactor with high resolution geometry and the position senstive detector at the D1B instrument stage of the Institut Laue Langevin, Grenoble. In preparation for this experiment we previously measured pole figures of an anorthosite (Wenk *et al.* 1985) and of an experimentally deformed limestone standard (Wenk *et al.* 1988), refining instrumentation and data processing. Details of the method are described in these papers.

In the present investigation several samples of mylonite rocks from Palm Canyon were first investigated by X-ray powder diffractometry to ascertain that patterns could be indexed and phases were identified. Subsequently the samples were chemically analyzed, normative compositions were calculated and a preliminary investigation of the preferred orientation of biotite was conducted (Kern & Wenk in press). Based on this, the three most suitable samples, a granodiorite protolith, a mylonite and a phyllonite, were selected.

The diffraction pattern of a composite of plagioclase, alkali feldspar, quartz and biotite is so complex that even using this sophisticated facility and applying peak deconvolution, resolution was difficult and we had to make some assumptions. We neglected alkali feldspar because it is a minor constituent and its preferred orientation is weak or similar to that of plagioclase. We could then single out 14 peaks in the spectrum, two for biotite, three for quartz, four for plagioclase and two overlapped peaks belonging to two phases (Fig. 3). The neutron

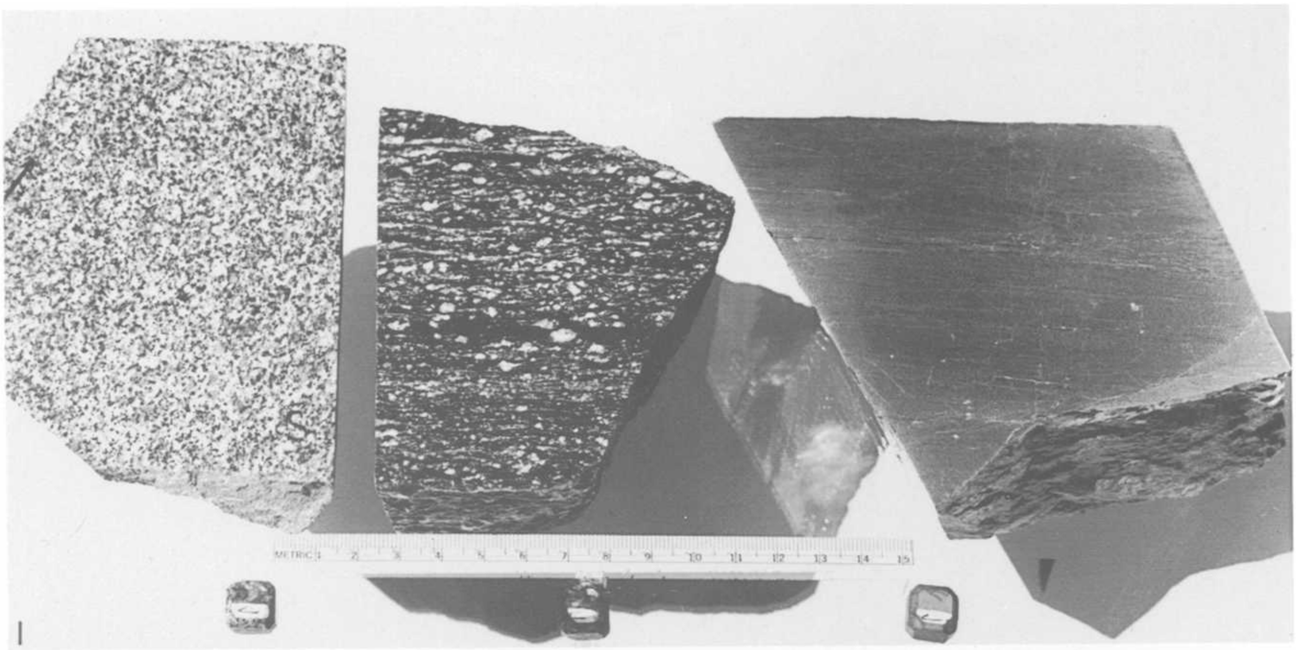

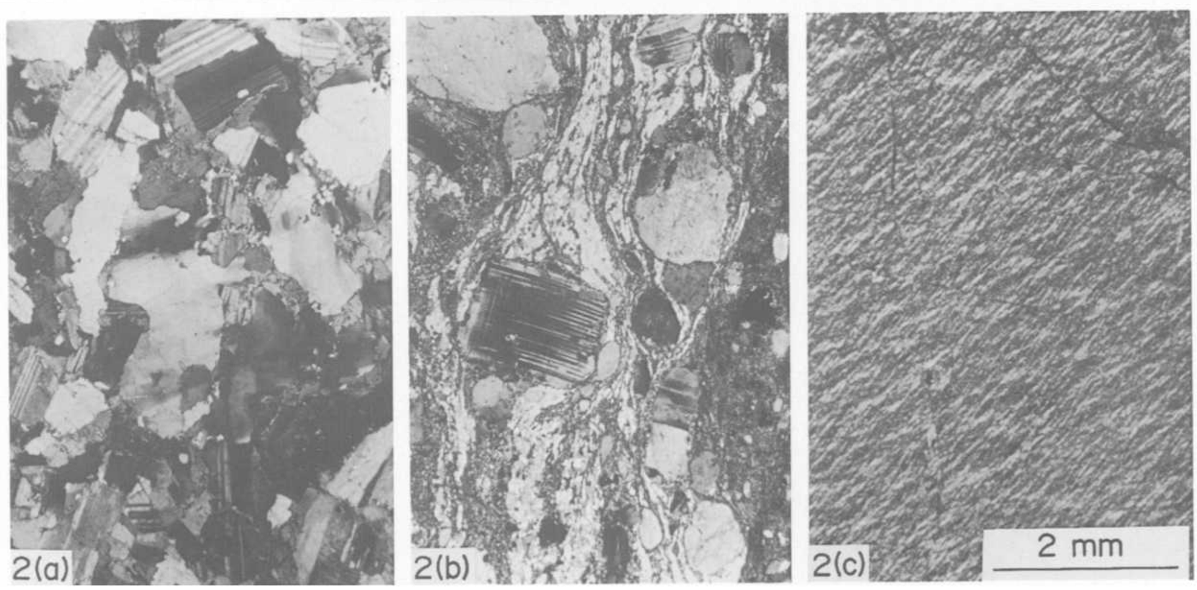

Fig. 1. Hand specimens of granodiorite (left), mylonite and phyllonite from the Santa Rosa mylonite zone, Palm Canyon, California. *X–Z* section parallel to the lineation. Small cubes were used for the diffraction experiments.

Fig. 2. Photomicrographs of granodiorite (PC 89), mylonite (PC 82) and phyllonite (PC 92) from the Santa Rosa mylonite zone. Same magnification for all. Crossed polars. Sections are normal to the foliation plane and contain the lineation.

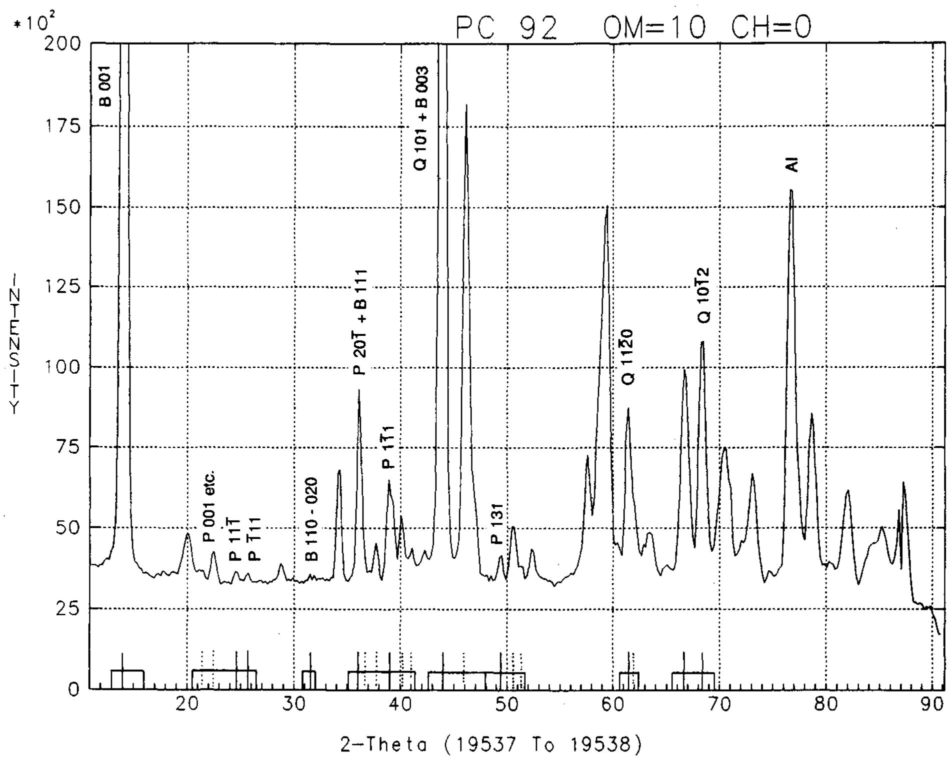

Fig. 3. Neutron diffraction spectrum of phyllonite PC 92. Some diffraction peaks used in the texture analysis are identified. Indicated at the bottom are regions of interest used in the peak deconvolution. B: biotite; Q: quartz; P: plagioclase; Al: aluminum sample holder.

radiation used had a wavelength of 2.5 Å and a flux of 6×10^6 n cm^{-2} s^{-1}. The detector has 400 cells spanning an arc of 80° in 2θ, i.e. five cells per degree. The sample is a cube with edges of 1 cm and rounded corners and edges (Fig. 1). For neutrons, absorption is minimal and has been neglected. We wanted to measure a maximum number of samples in the available time and therefore used rather short counting times (10 s) and a coarse grid on the pole figure. The undeformed granodiorite pole figures with weak texture were covered with 300 more or less equally spaced measurements, those of mylonite with 500 and those of phyllonite with 800, which turned out to be sufficient.

Due to relative intensity differences counting statistics were obviously better for some peaks than for others. Figure 4 shows stacks of selected profiles taken at 5° intervals from the center Z to the periphery X of the pole figure. Changes in peak intensity indicate differences in texture. They are minor in the case of undeformed granodiorite (PC 89) and a maximum in the case of phyllonite (PC 92). Consider for example the (001) biotite peak, which is strong in the center of the pole figure (Z, $\chi = 0°$) and vanishes toward the edge (X, $\chi = 90°$). The opposite is true for biotite (110). We also see at a glance that the texture of biotite is much stronger than that of quartz and feldspar. But for a more detailed texture description we need to deconvolute these profiles into pole figures.

The spectrum was divided into eight regions of interest, as indicated on Fig. 3, and then deconvoluted by a Gaussian fit, with peak location (2θ), half width and integrated intensity as variables. Poor convergence was apparent in large errors, and these data were rejected. It only involved a small number of measurements. Pole figures were constructed from the remaining intensity data. They are displayed in Figs. 5–7. Table 2 gives minimum and maximum values of the pole figures, in multiples of a random distribution.

RESULTS

Pole figures for biotite are shown in Fig. 5, those for quartz in Fig. 6 and those for plagioclase in Fig. 7. All are represented in equal-area projection. The distribution is normalized to express densities in multiples of a uniform distribution and contoured. We observe several features.

The statistics for quartz and feldspar in the undeformed granodiorite are inadequate, due to the coarse grain size, and those pole figures should not be interpreted.

The biotite (001) pole figure of granodiorite protolith displays a weak texture but the maximum is displaced from the center of the pole figure. We attribute this asymmetry to the difficulty in assigning mesoscopic fabric co-ordinates in the hand specimen.

(001) pole figures of biotite in the mylonite and the phyllonite compare well with those measured by O'Brien *et al.* (1987) by X-ray diffraction. This includes maximum pole densities and the slight but characteristic asymmetry of the texture peak.

Biotite (110) + (020) pole figures show concentrations in the foliation plane with a maximum in the lineation direction. The observation that [010] axes of phyllosilicate are not uniformly distributed in the foliation plane

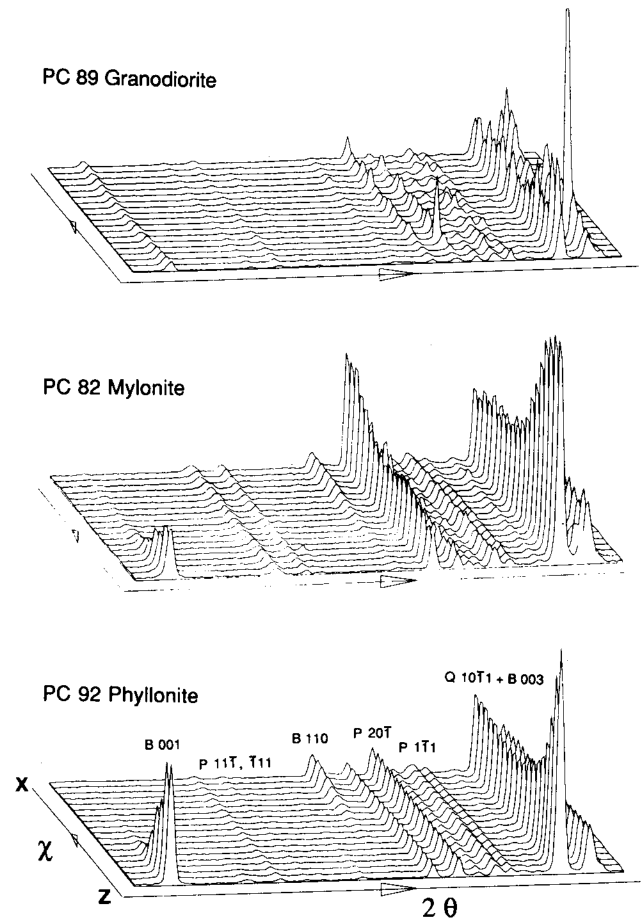

Fig. 4. Qualitative assessment of texture represented as stacks of diffraction spectra. The first spectrum is in the center of the pole figure ($Z, \chi = 0°$) corresponding to the pole of the foliation plane, the last spectrum ($X, \chi = 90°$) is perpendicular to it. B: biotite; Q: quartz; P: plagioclase.

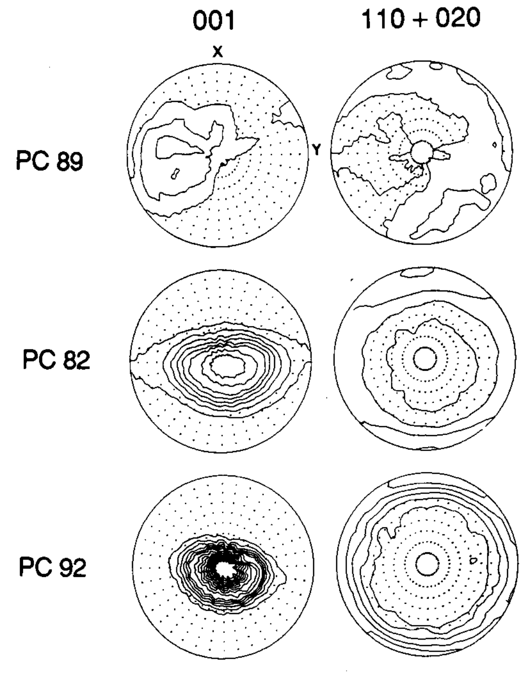

Fig. 5. Pole figures of biotite. Equal-area projection onto the foliation plane. The macroscopic lineation (X) is indicated. Contours are 0.5, 1, 1.5, 2, 2.5, 3, 4, . . ., 14 multiples of a random distribution (m.r.d.). Dotted below 1 m.r.d.

in the (001) plane, is new and appears significant. (It was not possible to separate the monoclinic [010] and [110] directions in this pseudo-hexagonal crystal.)

Quartz textures are best developed in the mylonite. The ($11\bar{2}0$) pole figure with three maxima on a great circle around the Y fabric direction is consistent with the typical mylonite 'single crystal' texture (e.g. Bunge & Wenk 1977, Erskine & Wenk 1985, Schmid & Casey 1986) and with [0001]-axes lying parallel to Y (in the foliation plane and normal to the lineation).

Most of the feldspar textures display irregularly disposed concentrations, and we do not give any significance to plagioclase pole figures in protolith and mylonite. However, in phyllonite a weak (the maxima do not exceed 1.3 multiples of a random distribution) but definite non-random pattern is present with monoclinic symmetry.

Table 2. Maxima and minima in pole figures in multiples of a random distribution (numbers in parentheses are unreliable due to poor grain statistics or peak overlaps)

	hkl	PC89	PC82	PC92
Biotite	001	2.3–0.5	5.8–0.0	14.5–0.0
	110	1.8–0.4	2.1–0.2	2.9–0.0
Quartz	$11\bar{2}0$	(2.5–0.4)	2.4–0.5	1.1–0.8
	$11\bar{2}1$	(1.6–0.3)	1.8–0.3	1.2–0.9
	$10\bar{1}2$	(1.9–0.4)	2.8–0.2	1.4–0.8
	$10\bar{1}1$(+)	(2.9–0.5)	2.3–0.3	(2.8–0.7)
Plagioclase	$\bar{1}11$	(2.7–0.4)	2.7–0.5	1.3–0.6
	$1\bar{1}1$	(2.6–0.4)	1.6–0.7	1.3–0.7
	$11\bar{1}$	(2.4–0.1)	1.3–0.7	1.3–0.5
	$\bar{1}31$	(2.3–0.3)	1.7–0.7	1.2–0.6
	$\bar{2}01$(+)	(2.9–0.1)	1.9–0.6	1.5–0.6

DISCUSSION

From texture data on only three samples we hesitate to draw general conclusions about texture development in deformed granitic rocks. We prefer to take this as an initial data base which needs to be augmented but the data are sufficiently new and interesting to warrant publication and discussion. We have demonstrated that it is feasible, though difficult, to measure pole figures in complex polyphase materials. The procedures which we have used are quite involved and time consuming and cannot be applied for routine analysis. Accessibility to the instruments is very limited and even after careful screening of samples, the deconvolution of the diffraction patterns is difficult. This is partially due to the large number of overlapping diffraction peaks for feldspar, and to the texture of biotite which is so strong that weak diffraction peaks from biotite can distort pole figures of quartz (e.g. $10\bar{1}1$) and plagioclase (e.g. $\bar{2}01$).

Nevertheless, some surprising results did emerge. During progressive mylonitization phyllosilicate textures become stronger. The study of O'Brien *et al.* (1987) indicates that they may reach a steady state with maximum (001) pole densities of 12–15 multiples of a random distribution (Means 1981). The fact that biotite [010] axes are oriented suggests that at least part of the deformation occurs by (001) ⟨010⟩ slip and is not solely a rigid body rotation of platelets which is consistent with TEM observation of Bell & Wilson (1981) and Goodwin & Wenk (in press).

Interestingly, the quartz texture develops in the mylonite stage but disappears again during further deformation. We attribute the quartz texture to recrystallization of a previous deformation texture by subgrain rotation (Poirier & Nicolas 1975), i.e. a dislocation-assisted process by which the original grain size is reduced by a factor of 10–100. The maximum of [0001] in the intermediate fabric direction coincides with the orientation of the most heavily deformed grains in self-consistent texture predictions (Wenk *et al.* in press) indicating that nucleation may be the controlling factor in selecting an orientation variant during recrystallization. The same texture type which we observe in these mylonitic granodiorites is present in the same rocks in local bands of pure quartz which is consistent with experimental observations of Dell'Angelo & Tullis (1986) that quartz behaves similarly in quartzites and in polymineralic rocks. Whereas $(11\bar{2}0)$ and $(11\bar{2}1)$ pole figures display nearly orthorhombic symmetry, the symmetry of the $(10\bar{1}1)$ and $(10\bar{1}2)$ pole figures is monoclinic. The symmetry axis is normal to the foliation plane and cannot therefore be interpreted as a simple shear texture with the foliation plane as the macroscopic shear plane and the lineation the shear direction. The fact that pole figures of rhombs display a different symmetry than those of hexagonal forms suggests that perhaps mechanical Dauphiné twinning in a different strain field is superposed on the initial orientation distribution (Tullis & Tullis 1972). At a more advanced stage of deformation, during phyllonitization, when grain size becomes uniformly fine and all phases are homogeneously distributed, preferred orientation almost vanishes. Interphase boundaries restrict movements of dislocations and boundary migration of quartz during recrystallization. A switch to boundary mechanisms such as grain-boundary sliding may reduce the texture.

Whereas the preferred orientation of plagioclase is weak in the mylonite stage with not much evidence for dislocation movements and no dynamic recrystallization (Ague 1988), it increases in the phyllonite stage. Unfortunately there is no microstructural evidence to indicate whether the texture develops by slip or by recrystallization (e.g. Tullis & Yund 1985). In contrast to the experiments of Tullis & Yund (1987) we did not observe significant preferred orientation development during the initial cataclastic stage in the mylonite when corners of grains are rounded and fine debris accumulates. The lack of preferred orientation is attributed to the fairly equiaxed grain shape of plagioclase in protolith, mylonite and phyllonite.

We find that in different minerals, different deformation processes occur at different stages of the deformation history, and a study of all phases in polymineralic rocks can give us much more information than the investigation of a single phase in a monomineralic rock. But at present we are not ready to apply a theory to predict texture development in such complex materials consisting of components of different grain size, grain shape and mechanical properties. The self consistent theory which has recently been applied to quartz (Wenk

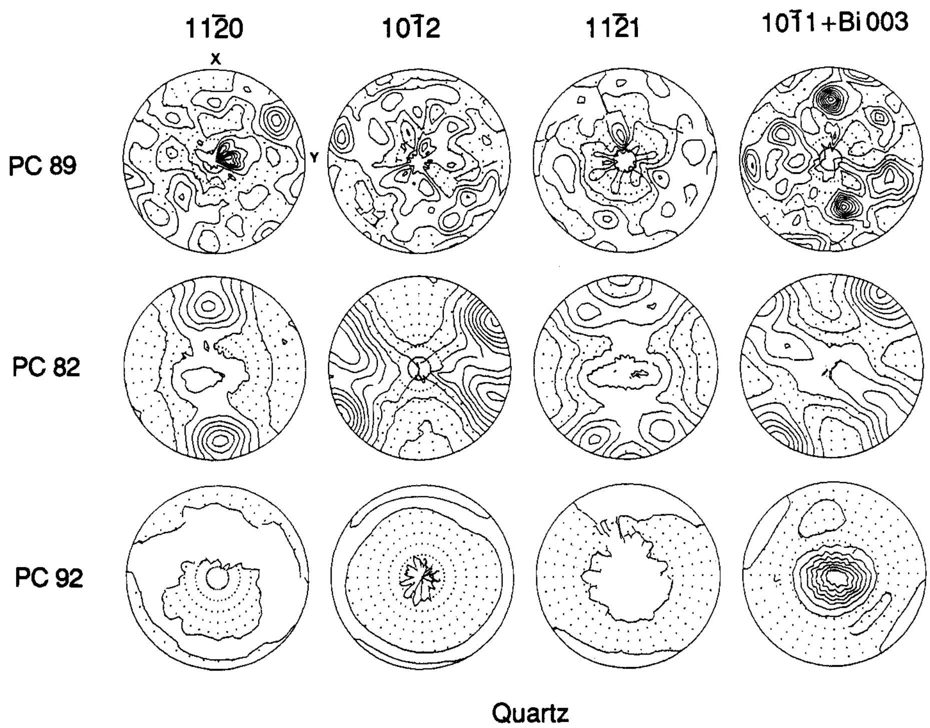

Fig. 6. Pole figures of quartz. Equal-area projection onto the foliation plane. The macroscopic lineation (X) is indicated. Contour interval 0.25 multiples of a random distribution (m.r.d.). Dotted below 1 m.r.d.

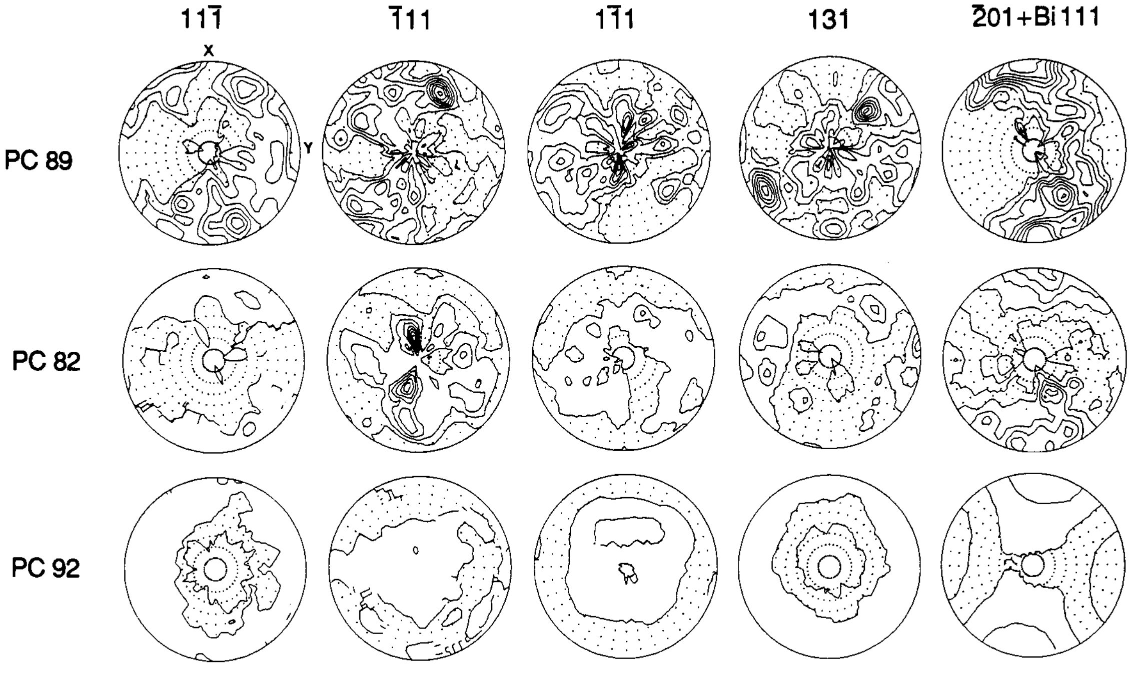

Fig. 7. Pole figures of plagioclase. Equal-area projection onto the foliation plane. The macroscopic lineation (X) is indicated. Contour interval 0.25 multiples of a random distribution (m.r.d.). Dotted below 1 m.r.d.

et al. in press) has potential, but it will be necessary to have experimental data to test theories and such data are not yet available.

Acknowledgements—We are grateful to S. Schmid and J. Tullis for constructive reviews which improved the manuscript and to L. Goodwin for XRF analyses. H.-R. Wenk acknowledges support from the A. v. Humboldt Foundation during a sabbatical leave at T.U. Hamburg-Harburg, from NSF through grants EAR-8416938 and EAR-8709378, and IGPP Los Alamos. We are appreciative for access to the facilities at ILL, Grenoble.

REFERENCES

Ague, D. 1988. Natural deformation of plagioclase: a microstructural investigation. Unpublished Ph.D. thesis, University of California, Berkeley.

Bell, I. A. & Wilson, C. J. L. 1981. Deformation of biotite and muscovite: TEM microstructure and deformation model. *Tectonophysics* **78**, 201–228.

Bunge, H. J. & Wenk, H.-R. 1977. Three-dimensional texture analysis of three quartzites (trigonal crystal and triclinic specimen symmetry). *Tectonophysics* **40**, 257–285.

Dell'Angelo, L. N. & Tullis, J. 1986. A comparison of quartz *c*-axis preferred orientations in experimentally deformed aplites and quartzites. *J. Struct. Geol.* **8**, 683–692.

Dingley, D. J. 1987. On line microtexture determination using backscatter Kikuchi diffraction in a scanning electron microscope. In: *Proc. 8th Int. Conf. Textures of Materials* (edited by Kallend, J. S. & Gottstein, G.). Metall. Soc., Warrendale, Pennsylvania, 189–194.

Erskine, B. C. & Wenk, H.-R. 1985. Evidence for late Cretaceous crustal thinning in the Santa Rosa mylonite zone, southern California. *Geology* **13**, 274–277.

Goodwin, L. B. & Wenk, H.-R. In press. Intracrystalline folding and cataclasis in biotite of the Santa Rosa mylonite zone: HVEM and TEM observations. *Tectonophysics.*

Kern, H. & Wenk, H.-R. In press. Fabric related velocity anisotropy and shear wave splitting in rocks from the Santa Rosa mylonite zone, California. *J. geophys. Res.*

Lloyd, G. E. & Ferguson, C. C. 1986. A spherical electron channelling pattern map for use in quartz petrofabric analysis. *J. Struct. Geol.* **8**, 517–526.

Means, W. D. 1981. The concept of steady-state foliation. *Tectonophysics* **78**, 179–199.

O'Brien, D. K., Wenk, H.-R., Ratschbacher, L. & You, Z. 1987. Preferred orientation of phyllosilicates in phyllonites and ultramylonites. *J. Struct. Geol.* **9**, 719–730.

Poirier, J. P. & Nicolas, A. 1975. Deformation induced recrystallization due to progressive misorientation of subgrains, with special reference to mantle peridotites. *J. Geol.* **83**, 707–720.

Schmid, S. M. & Casey, M. 1986. Complete fabric analysis of some commonly observed quartz *c*-axis patterns. In: *Mineral and Rock Deformation: Laboratory Studies* (edited by Hobbs, B. E. & Heard, H. C.). *Am. Geophys. Un. Geophys. Monogr.* **36**, 263–286.

Schwarzer, R. A. & Weiland, H. 1988. Texture analysis by the measurement of individual grain orientations—electron microscopical methods and applications on dual phase steel. *Textures Microstruct.* **819**, 551–557.

Simpson, C. & Wintsch, R. P. 1989. Evidence for deformation-induced K-feldspar replacement by myrmekite. *J. metamorphic Geol.* **7**, 261–275.

Taylor, G. 1938. Plastic strain in metals. *J. Inst. Metall.* **62**, 307–324.

Tullis, J. & Tullis, T. E. 1972. Preferred orientation produced by mechanical Dauphiné twinning: thermodynamics and axial experiments. In: *Flow and Fracture of Rocks* (edited by Heard, H. C. *et al.*). *Am. Geophys. Un. Geophys. Monogr.* **16**, 67–82.

Tullis, J. & Yund, R. A. 1985. Dynamic recrystallization of feldspar: a mechanism for ductile shear zone formation. *Geology* **13**, 238–241.

Tullis, J. & Yund, R. A. 1987. Transition from cataclastic flow to dislocation creep of feldspar: mechanisms and microstructures. *Geology* **15**, 606–609.

Wenk, H.-R., Bunge, H. J., Jansen, E. & Pannetier, J. 1985. Preferred orientation of plagioclase—neutron diffraction and U-stage data. *Tectonophysics* **126**, 271–284.

Wenk, H.-R., Canova, G., Molinari, A. & Kocks, U. F. In press. Viscoplastic modeling of texture development in quartzite. *J. geophys. Res.*

Wenk, H.-R., Kern, H., Pannetier, J., Höfler, S., Schaefer, W., Will, G. & Brokmeier, H. G. 1988. Neutron diffraction texture analysis: Standard project (preliminary results). In: *Proc. 8th Int. Conf. Textures of Materials* (edited by Kallend, J. S. & Gottstein, G.). Metall. Soc., Warrendale, Pennsylvania, 229–234.

Wenk, H.-R., Kern, H., Schaefer, H. & Will, G. 1984. Comparison of X-ray and neutron diffraction in texture analysis of carbonate rocks. *J. Struct. Geol.* **6**, 687–692.